Loss of Binocular Vision in Monocularly Blind Patients Causes Selective Degeneration of the Superior Lateral Occipital Cortices

Doety Prins, Nomdo M. Jansonius, and Frans W. Cornelissen

Laboratory of Experimental Ophthalmology, Department of Ophthalmology, University of Groningen, University Medical Center Groningen, Groningen, The Netherlands

Correspondence: Doety Prins, Laboratory of Experimental Ophthalmology, Department of Ophthalmology, University of Groningen, University Medical Center Groningen, PO Box 30.001, HPC BB61, 9700 RB Groningen, The Netherlands;
d.prins@umcg.nl.
Frans W. Cornelissen, Laboratory of Experimental Ophthalmology, Department of Ophthalmology, University of Groningen, University Medical Center Groningen, PO Box 30.001, HPC BB61, 9700 RB Groningen, The Netherlands;
f.w.cornelissen@umcg.nl.

Submitted: July 27, 2016
Accepted: January 27, 2017

Citation: Prins D, Jansonius NM, Cornelissen FW. Loss of binocular vision in monocularly blind patients causes selective degeneration of the superior lateral occipital cortices. *Invest Ophthalmol Vis Sci*. 2017;58:1304–1313. DOI:10.1167/iovs.16-20404

Purpose. Chronic ocular pathology, such as glaucoma and macular degeneration, is associated with neuroanatomic changes in the visual pathways. It is a challenge to determine the mechanism responsible for these changes. This could be functional deprivation or transsynaptic degeneration. Acquired monocular blindness provides a unique opportunity to establish which mechanism underlies neuroanatomic changes in ocular pathology in general, since the loss of input is well defined, and it causes selective functional deprivation due to the loss of stereopsis. Here, we assessed whether acquired monocular blindness is associated with neuroanatomic changes, and if so, where these changes are located.

Methods. High-resolution T1-weighted magnetic resonance images were obtained in 15 monocularly blind patients and 18 healthy controls. We used voxel- and surface-based morphometry to compare gray and white matter volume, cortical thickness, mean curvature, and surface area between these groups.

Results. The gray matter volume in the bilateral superior lateral occipital cortices was decreased in the monocular blind patients, in the absence of volumetric differences in their early visual cortex.

Conclusions. The volumetric decrease in the superior lateral occipital cortices is consistent with specific functional deprivation, as the superior lateral occipital cortices play an important role in depth perception. Moreover, in the absence of differences in the early visual cortex, the decrease is inconsistent with transsynaptic degeneration propagating from the degenerated retinal axons.

Keywords: monocular blindness, functional deprivation, visual cortex

Treatment of blindness is the ultimate challenge in ophthalmology; it has motivated the development of various vision restoration therapies including retinal implants, stem-cell–derived retinal pigment epithelium, and gene therapy.[1–4] The potential success of such future treatments will depend to a great extent on the capacity of the brain to guide and process the new input following vision restoration. Previous studies[5–13] have found evidence for neuroanatomic changes in patients with various eye diseases. Owing to such changes, the brain may no longer be able to optimally process new input from a retinal implant. As for a truly successful treatment it needs to be able to do so, it is important to understand the mechanism underlying the association between prolonged partial blindness and neuroanatomic changes.

Three mechanisms may explain the association between loss of visual input and neuroanatomic changes. First, in functional deprivation a permanent loss of visual input (information) from the eye leads to diminished activity in the corresponding parts of the visual pathways and cortex, which, in turn, leads to neuroanatomic degeneration. Accordingly, the degeneration will be located specifically in the section or region of the visual system that previously processed the concerning information. Second, in transsynaptic degeneration, the degenerating axons originating from the eye provoke degeneration of the directly connected neurons, and this degeneration is propagated toward more posterior parts of the visual pathways, and may eventually also reach the visual cortex. Specific to transsynaptic degeneration is that it predicts a continuous link of degeneration to the damaged axons at the level of the eye. Distinguishing between the contributions of these two mechanisms has been problematic, as neural and functional visual losses are usually highly correlated and difficult to characterize. Third, there are indications that degenerative eye diseases, such as macular degeneration and glaucoma, are associated with generalized neurodegenerative diseases, such as Alzheimer's disease.[14–19] As such, the neuroanatomic changes might not exclusively be caused by functional deprivation or transsynaptic degeneration, but could be due to the general neurodegenerative character of the disease.

Studying patients with previously healthy eyes who became monocularly blind—due to, for example, an eye trauma—provides a unique opportunity to disentangle the possible causes of the association between altered visual function and neuroanatomic changes. Unlike in chronic ocular pathology, in this group the reduction of visual input is well defined. Moreover, monocular blindness causes a loss of binocular vision and stereopsis, resulting in a highly selective functional deprivation. Finally, there is no association with neurodegen-

Copyright 2017 The Authors

This work is licensed under a Creative Commons Attribution-NonCommercial-NoDerivatives 4.0 International License.

Downloaded from iovs.arvojournals.org on 10/17/2019

erative diseases. If we can determine whether and where neuroanatomic changes occur in monocularly blind patients, we would gain more insight into the etiology of neuroanatomic changes associated with visual loss in general. In contrast to bilateral blindness—which has been studied extensively[20–32]—systematic research into neuroanatomic changes associated with monocular blindness is scarce.[33–35]

The aim of our study was to determine whether and how monocular blindness affects the neuroanatomic properties of the visual pathways. Such neuroanatomic properties were defined by gray and white matter volume, cortical thickness, surface area, and mean curvature.

Materials and Methods

Ethics Statement

The Medical Ethical Committee of the University Medical Center Groningen approved this study. The study conformed to the tenets of the Declaration of Helsinki. All subjects gave their written informed consent before participating in the study.

Subjects

Initially, 15 monocularly blind patients and 20 healthy subjects (controls) responded to our invitation to participate. As the controls were on average older, we removed controls, starting with the oldest, until the groups had the same mean age. This resulted in 15 monocularly blind patients and 18 controls. The inclusion criteria for the monocularly blind patients were the following. They had to be unilaterally light-perception negative for at least 5 years (mean: 21 years), due to a trauma ($n = 11$, in 11 patients the eye was removed) or after surgery for a tumor ($n = 4$, in 3 patients the eye was removed). The contralateral eye had to have a good visual acuity (0.8 or better) and an intact visual field. Healthy controls had to have a good visual acuity and intact visual field in both eyes. None of the subjects had previously been diagnosed with neurologic disorders, psychiatric disorders, or any degenerative ocular disease.

The monocularly blind patients had a mean age of 63 years (range, 54–72 years); 47% of them were males. The healthy controls had a mean age of 62 years (range, 53–75 years); 61% of them were males. In the group of monocularly blind patients, seven patients were blind in their right eye, and eight were blind in their left eye. Both groups had the same mean (SD) visual acuity (1.1 [0.17] in the patients and 1.1 [0.16] in the controls, [$P = 0.73$]).

Data Acquisition

Magnetic resonance (MR) images of all subjects were obtained on a 3.0 Tesla magnetic resonance imaging (MRI) scanner (Philips Intera, Eindhoven, The Netherlands) at the Neuroimaging Center of the University Medical Center Groningen. Whole brain T1-weighted images with a voxel dimension of $1 \times 1 \times 1$ mm were acquired by using a sequence of T1W/3D/FFE, 30° flip angle, repetition time 25 ms, matrix size 256×256, and field of view $256 \times 160 \times 204$, yielding 160 slices.

The visual acuity was measured with a Snellen chart with optimal correction for the viewing distance. The visual field was tested with frequency-doubling technology (C20-1 screening mode).

Data Analysis

We analyzed the anatomic properties of the visual pathways by using voxel-based morphometry (VBM) and surface-based morphometry (SBM). Voxel-based morphometry was used to study the volume of the gray and white matter; SBM was used to study the cortical thickness, surface area, and gyrification pattern. The gyrification is an index of the amount of cortex that is covered within the sulcal folds, compared to the amount of cortex on the outer cortex; the index increases with more extensive folding of the cortex.

Voxel-Based Morphometry Analysis. We performed VBM analysis of the gray matter and white matter volume by using the FMRIB Software Library (FSL) analysis tools (version 5.0.6; http://www.fmrib.ox.ac.uk/fsl, available in the public domain).[36,37] First, we applied nonlinear noise reduction by using Smallest Univalue Segment Assimilating Nucleus (SUSAN). Second, we segmented the brain from nonbrain tissue, using the Brain Extraction Tool (BET).[38] Subsequently, we performed bias field correction and segmented the brain into gray matter, white matter, and cerebrospinal fluid with the FMRIB Automated Segmentation Tool (FAST) from the Oxford Centre for Functional Magnetic Resonance Imaging of the Brain.[39] We registered all the images to the template of the Montreal Neurological Institute (MNI template) with the FMRIB Linear Image Registration Tool (FLIRT) and the FMRIB Non-linear Image Registration Tool (FNIRT), and applied the registration to the gray and white matter segments.[40,41] The images were modulated to compensate for local expansion. Using the FSL "randomise" analysis tool, we performed nonparametric permutation tests on our data.[42] With VBM, it is possible to measure concentration of gray or white matter (i.e., the proportion of gray or white matter relative to other tissue types within a region) or volume (i.e., the absolute amount of gray or white matter in different regions). In our study, we chose to focus on volume, as neurodegeneration predicts a change in the absolute amount of gray and white matter.

Surface-Based Morphometry Analysis. We performed SBM analysis of cortical thickness, mean curvature, surface area, and gray matter volume by using Freesurfer (version 5.3.0; http://surfer.nmr.mgh.harvard.edu/, available in the public domain). We digitally removed the nonbrain tissue[43] and performed automated Talairach transformation and intensity normalization.[44] Subsequently, tessellation of the gray/white and gray/cerebrospinal fluid boundaries and automatic correction of topologic inaccuracies was performed, which we customized by setting the value for the lower threshold of the white matter to an appropriate value for our dataset.[45,46] The process continued with surface deformation and inflation,[47,48] registration to a spherical atlas,[49] and automatic parcellation of the cortex surface based on gyral and sulcal organization.[50,51]

Region of Interest (ROI) Analysis. In the ROI-based analyses, we used masks of the various gray and white matter structures of the visual pathways. Figure 1 presents the ROIs: the pregeniculate structures, which contain the optic nerves, chiasm and optic tracts, the lateral geniculate bodies, the optic radiations, the calcarine region, the occipital pole, the inferior lateral occipital cortices, and the superior lateral occipital cortices. The masks for the pregeniculate structures were created manually and adjusted to match the structures in each individual subject if needed. The masks for the lateral geniculate bodies and for the optic radiations were obtained from the Jülich histologic atlas.[52,53] The masks for the calcarine region, the occipital pole, the inferior lateral occipital cortices, and the superior lateral occipital cortices were obtained from the Harvard-Oxford cortical structural atlas.[50] All ROIs were defined in FSL.

We chose the ROIs on the basis of anatomy of the visual pathways and on the basis of approximate location of regions that process binocular signals in the dorsal stream. We defined the ROIs of the occipital pole and pericalcarine cortices to

Investigative Ophthalmology & Visual Science

Downloaded from iovs.arvojournals.org on 10/17/2019

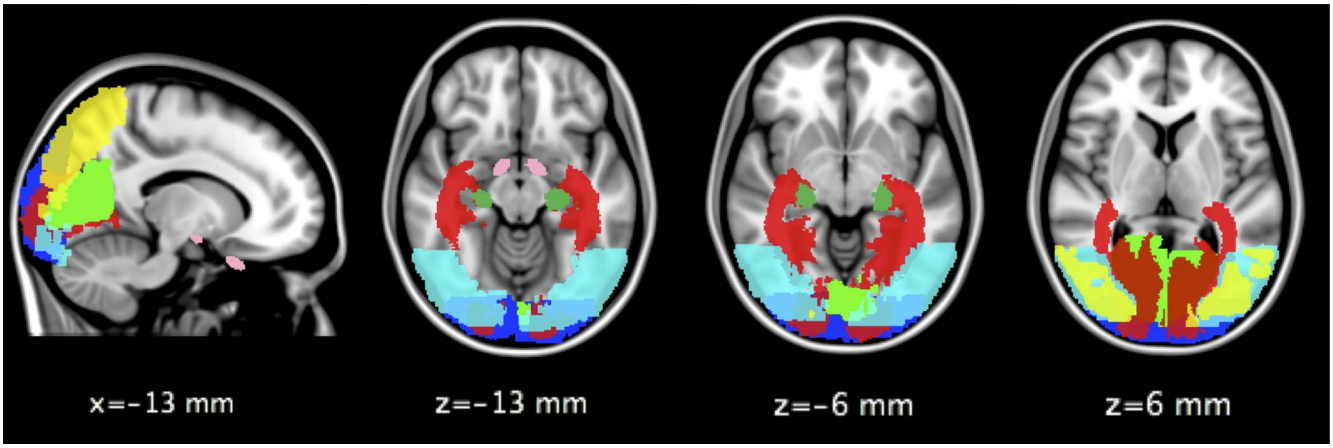

FIGURE 1. Regions of interest along the visual pathway. *Pink*: pregeniculate structures; *dark green*: lateral geniculate bodies; *red*: optic radiations; *lighter green*: pericalcarine cortices; *dark blue*: occipital pole; *lighter blue*: inferior lateral occipital cortex; *yellow*: superior lateral occipital cortex. The Talairach position of the slices is given by their "*x*" and "*z*" values.

distinguish between central and peripheral vision. The ROI of the superior lateral occipital cortex was added, as it comprises part of the dorsal visual stream. The ROI of the inferior lateral occipital cortex was added to have equivalent counterpart that comprises part of the ventral visual stream.

In all these ROIs, we analyzed the volume of the gray matter and white matter by using VBM. In the calcarine region, the occipital pole, the inferior lateral occipital cortices, and the superior lateral occipital cortices, we also analyzed cortical thickness, gyrification, and surface area by using SBM.

Statistics. We examined differences between monocularly blind patients and healthy controls by using multivariate analysis of covariance (IBM [Armonk, NY, USA] SPSS Statistics software package, version 20). The white matter volume, gray matter volume, cortical thickness, gyrification pattern, and surface area for each ROI were included as dependent variables, and the subject groups were entered as a fixed factor. We added age as a covariate in the analysis. The threshold for significance in the ROI analyses was set to a P value of 0.05 (uncorrected).

Region of Interest Analysis of Optic Nerves. Since not all monocularly blind patients had their blind eye on the same side, we performed the ROI analyses in two stages. In the first analysis, we compared the volumes of the optic nerves between monocularly blind patients and healthy controls. This analysis was done separately for the monocularly blind patients with a blind right eye and for the monocularly blind patients with a blind left eye, in both cases comparing them to all the healthy controls.

Region of Interest Analysis of Postchiasmal Structures. The nerve fibers that carry the information from the homonymous hemifields of both eyes to the visual cortex are combined after the chiasm. Hence, no detectable volumetric differences in the postchiasmal structures were expected between the monocularly blind patients with a blind right eye and those with a blind left eye. Therefore, in a second analysis, we compared the visual pathway structures onwards from the optic chiasm to the posterior parts of the visual pathways, this time for the entire group of monocularly blind patients and again comparing them to the healthy controls.

Exploratory Whole-Brain Analysis. To determine the presence of unexpected differences in the neuroanatomy between monocularly blind patients and healthy controls, we performed additional exploratory whole-brain analyses by using both VBM and SBM. With VBM, we compared gray and white matter volume, while with SBM, we compared the cortical thickness and mean curvature across the entire brain. In both cases, age was added as a covariate.

Comparisons were made after applying a familywise error correction for multiple comparisons ($P < 0.05$).

RESULTS

In summary, we found a significantly smaller volume of the optic nerve on the side of the blind eye, the optic chiasm, the bilateral optic tracts, and the bilateral superior lateral occipital cortices in monocularly blind patients than healthy controls. We will describe these results in more detail below.

Region of Interest Analyses

Voxel-Based Morphometry ROI Analysis of the Optic Nerves. To compare the white matter volume of the optic nerves of the monocularly blind patients to that of the healthy controls, we performed VBM analyses in two subgroups. Table 1 lists the results of these analyses. On the one hand, in the patients with a blind right eye, the right optic nerve showed a significant decrease in volume, whereas the left optic nerve did not. On the other hand, in the patients with a blind left eye, the left optic nerve showed a significant decrease in volume, whereas the right optic nerve did not. Figure 2 visualizes the location of these volumetric differences in the optic nerves for the patients with either a blind right eye (Fig. 2a) or a blind left eye (Fig. 2b).

Voxel-Based Morphometry ROI Analysis of the Visual Pathways From the Optic Chiasm Toward the Visual Cortex. This time including the entire group of monocularly blind patients, we performed ROI analyses of the optic chiasm, the optic tracts, the lateral geniculate bodies, the optic radiations, the calcarine region, the occipital pole, the inferior lateral occipital cortices, and the superior lateral occipital cortices. Table 2 and the first row of Table 3 show the results of these analyses and highlight the ROIs for which we found significant reductions in white or gray matter volume: the optic chiasm, the bilateral optic tracts, and the bilateral superior lateral occipital cortices. We did not find any significant differences in gray matter volume in the pericalcarine region and the occipital pole. Figure 3 visualizes the volumetric differences in the optic tracts (Fig. 3a) and the visual cortex (Fig. 3b). The results of this latter VBM analysis of the gray matter are also visualized on the cortical surface, as shown in Figure 4. Gray matter volume was significantly reduced

Investigative Ophthalmology & Visual Science

Downloaded from iovs.arvojournals.org on 10/17/2019

Table 1. ROI Morphometric Values (μ ± σμ) of the Optic Nerves

Volume, mm³	Right Optic Nerve	Left Optic Nerve
Monocular blind OD	27 ± 5	125 ± 6
Monocular blind OS	144 ± 18	13 ± 4
Healthy controls	141 ± 12	136 ± 12
Monocular blind OD		
f value (*df* = 1,22)	31.890	0.335
P value	<0.001*	0.57
Monocular blind OS		
f value (*df* = 1,23)	0.019	44.240
P value	0.89	<0.001*

White matter volumes of the right and the left optic nerve for the subgroups of monocular blind patients with either a blind right eye or a blind left eye, and the healthy controls. *df*, degrees of freedom; OD, oculus dexter (right eye); OS, oculus sinister (left eye); μ, mean; σμ, standard error of the mean.

* Significant difference between the patient group and the control group.

bilaterally in the superior lateral occipital cortices. We found no evidence for a reduced white matter volume of the optic radiations. However, within the optic radiations we did find relatively small sections of significantly increased white matter volume.

Surface-Based Morphometry ROI Analysis of the Visual Cortex. We performed SBM analyses in the ROIs of the pericalcarine cortices, the occipital pole, the inferior lateral occipital cortices, and the superior lateral occipital cortices. Table 3 indicates that in none of these ROIs did cortical thickness, mean curvature, or surface area (second, third, and fourth row of Table 3, respectively) differ significantly between the monocularly blind patients and the healthy controls.

Exploratory Whole-Brain Analyses

Using whole-brain analyses, we examined whether unexpected neuroanatomic differences might be present beyond the previously examined visual pathway ROIs. However, we found no significant differences in either the gray or the white matter, or in cortical thickness or mean curvature.

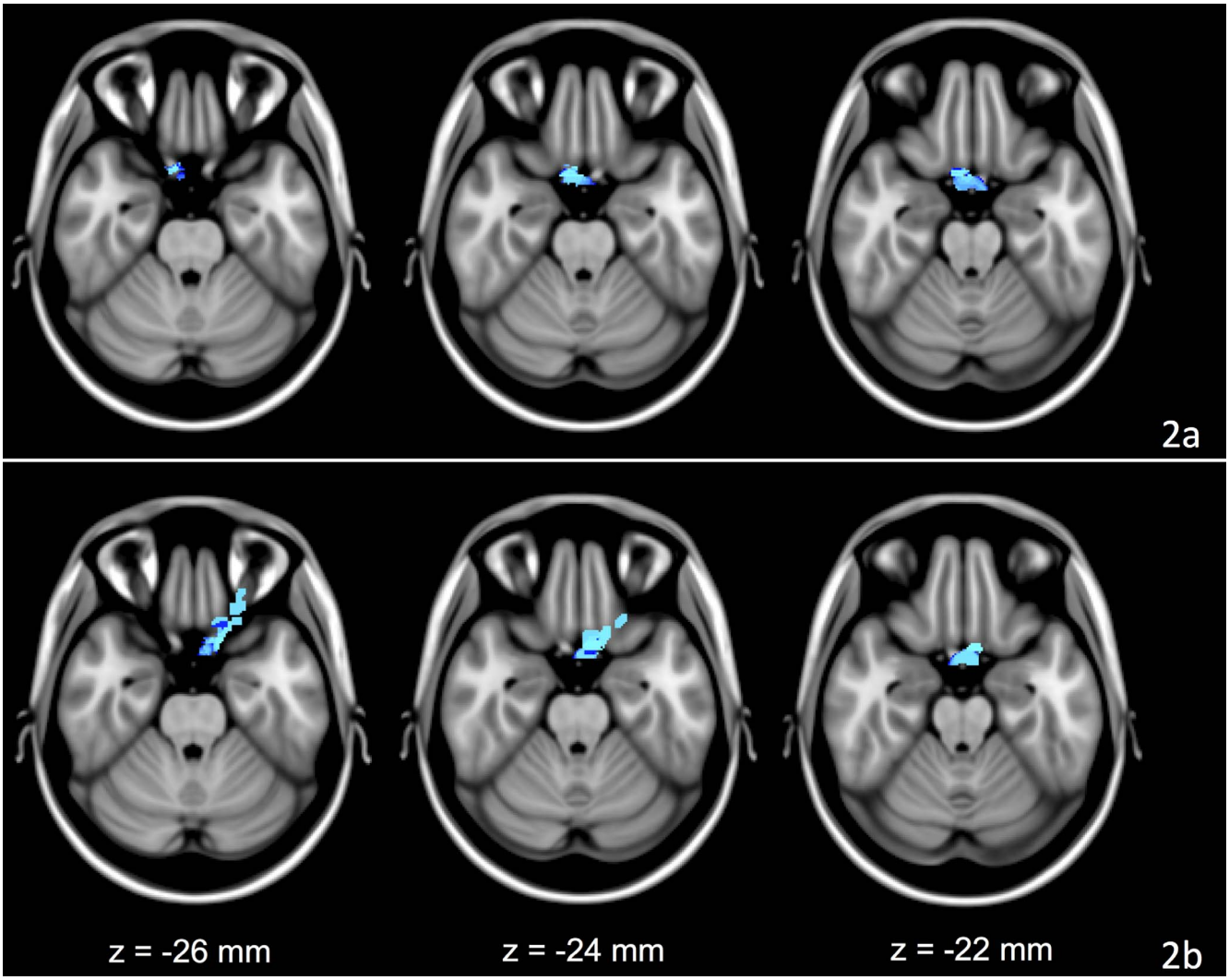

Figure 2. Volumetric differences in the optic nerve and the optic chiasm ROIs. (**a**) The areas in *blue* highlight where the monocularly blind patients with a blind right eye show significantly lower volume in the ROI of the right optic nerve than the healthy controls ($P < 0.05$, uncorrected). (**b**) The areas in *blue* highlight where the monocular blind patients with a blind left eye show significantly lower volume in the ROI of the left optic nerve than the healthy controls ($P < 0.05$, uncorrected). The Talairach position of the slices is given by their "*z*" values. Regions of interest are defined in Figure 1.

Investigative Ophthalmology & Visual Science

Downloaded from iovs.arvojournals.org on 10/17/2019

Table 2. ROI Morphometric Values (μ ± σμ) of Chiasm, Optic Tracts, Lateral Geniculate Bodies, and Optic Radiations

Volume, mm³	Chiasm	Optic Tracts	Lateral Geniculate Bodies	Optic Radiations
Monocular blind	119 ± 12	504 ± 17	1,052 ± 38	128,956 ± 554
Healthy controls	247 ± 10	570 ± 13	1,037 ± 34	128,211 ± 525
f value (*df* = 1,30)	70.151	10.213	0.081	1.145
P value	<0.001*	0.003*	0.78	0.29

* Significant difference between the patient group and control group.

Discussion

We found that binocular vision loss—as a result of acquired monocular blindness—is associated with a reduced volume of the superior lateral occipital cortices. Functionally, the location of this degeneration is consistent with the loss of binocular vision and stereopsis in the monocularly blind patients. Moreover, in the absence of accompanying volumetric reductions of the early visual cortex, this implies that the cortical degeneration can only be explained by functional deprivation and not by propagated transsynaptic degeneration that originated at an earlier stage along the visual pathway.

Volumetric Loss in the Dorsal Visual Stream

We found gray matter volumetric decreases in the bilateral superior lateral occipital cortices. The superior lateral occipital cortices are located in the dorsal visual stream, which processes information about the location of objects in space. Stereopsis is needed to perceive depth and to precisely localize objects in space. Several functional MRI (fMRI) studies have shown that dorsal visual areas are involved in stereoscopic depth perception, specifically the dorsal V3.[54–63] Furthermore, the area in which we found the gray matter volumetric decrease extends to the posterior part of the intraparietal sulcus, which has been implicated in visual attention and eye movements.[64] Since monocularly blind patients can only scan the outside world using one eye, they may have adjusted to a different pattern of eye movements. Therefore, the decrease in gray matter volume in the superior lateral occipital cortices in monocularly blind patients might be explained by both the loss of stereopsis as well as accompanying changes in oculomotor behavior. Irrespective, this volumetric decrease in the superior lateral occipital cortices is particularly significant, as we found no evidence for neuroanatomic changes in the early visual cortex.

Such a "skipping of one or more synapses" is the primary marker that can distinguish between explanations based on functional deprivation and transsynaptic degeneration. There is strong evidence that deprivation due to visual field defects (e.g., due to glaucoma or AMD) results in extensive degeneration at the level of the cortex and optic radiations.[5,6,8,65–68] However, in such cases, the functional deprivation and transsynaptic degeneration accounts predict the exact same pattern of results. As we mentioned in our introduction, this is not the case in the monocular blind observers, which is why this is such an important group to study. In monocular blindness, we do find clear indications of degeneration at the level of the pregeniculate structures (see also the next section), but not immediately beyond. The absence of degeneration in the early visual cortex cannot be due to a lack of time for transsynaptic degeneration to have occurred. On average, the monocular blind observers were known as such for 21 years. Hence, these results imply that the observed differences in the dorsal stream are the exclusive result of functional deprivation rather than transsynaptic degeneration.

Table 3. ROI Morphometric Values (μ ± σμ) of the Pericalcarine Cortices, Occipital Pole, and the Inferior and Superior Lateral Occipital Cortices

Anatomical Property	Pericalcarine Cortices	Occipital Pole	Inferior Lateral Occipital Cortices	Superior Lateral Occipital Cortices
Volume, mm³				
Monocular blind	15,691 ± 408	31,119 ± 831	30,860 ± 955	62,957 ± 1,559
Healthy controls	15,669 ± 402	32,288 ± 719	32,634 ± 648	66,604 ± 1,354
f value (*df* = 1,30)	0.000	1.352	2.894	5.522
P value	0.99	0.25	0.099	0.026*
Cortical thickness, mm				
Monocular blind	3.03 ± 0.03	2.99 ± 0.03	3.30 ± 0.04	3.12 ± 0.05
Healthy controls	3.02 ± 0.05	2.98 ± 0.03	3.25 ± 0.04	3.08 ± 0.04
f value (*df* = 1,30)	0.015	0.017	0.865	0.669
P value	0.90	0.90	0.36	0.42
Mean curvature, mm^{-1}				
Monocular blind	0.15 ± 0.002	0.16 ± 0.003	0.15 ± 0.002	0.14 ± 0.003
Healthy controls	0.15 ± 0.003	0.16 ± 0.003	0.15 ± 0.003	0.14 ± 0.003
f value (*df* = 1,30)	0.062	1.090	0.240	0.316
P value	0.81	0.31	0.63	0.58
Surface area, mm²				
Monocular blind	6,838 ± 275	12,387 ± 496	15,093 ± 678	20,666 ± 900
Healthy controls	7,112 ± 202	12,510 ± 338	14,737 ± 399	20,148 ± 508
f value (*df* = 1,30)	0.651	0.045	0.213	0.268
P value	0.43	0.83	0.65	0.61

* Significant difference between the patient group and control group.

Investigative Ophthalmology & Visual Science

Downloaded from iovs.arvojournals.org on 10/17/2019

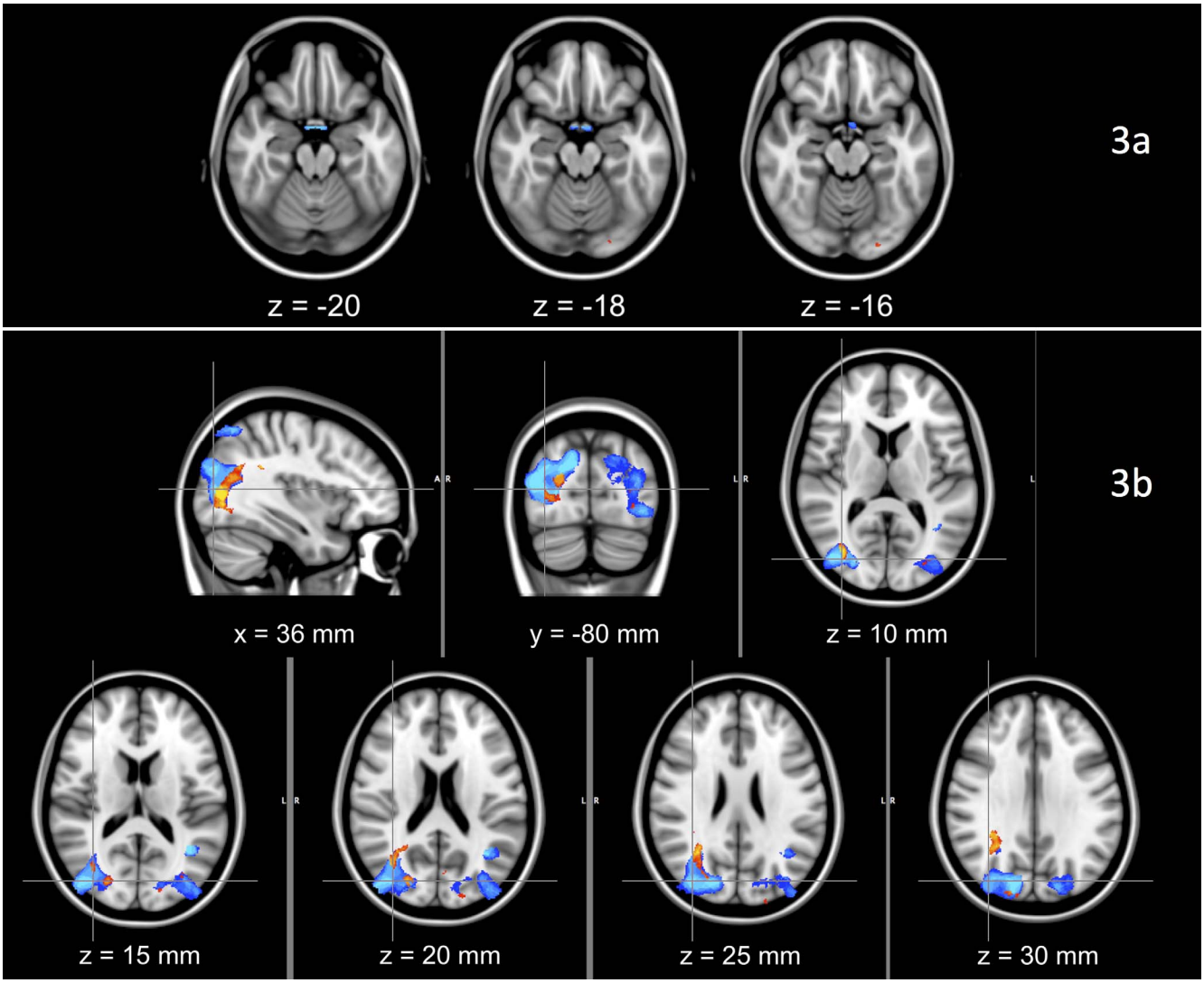

FIGURE 3. Volumetric differences in the optic chiasm, the optic tract, the optic radiation, and the visual cortex ROIs. (**a**) The areas in *blue* highlight where the monocularly blind patients show significantly lower volume in the ROIs in the optic chiasm and the optic tracts (see Fig. 1) than the healthy controls ($P < 0.05$, uncorrected). (**b**) The areas in *blue* highlight where the monocular blind patients show significantly lower gray matter volume in the ROIs in the visual cortex than the healthy controls. The *red-yellow* areas highlight where the monocular blind patients show significantly higher white matter volume in the ROIs of the optic radiations than the healthy controls ($P < 0.05$, uncorrected). Talairach position of the slices is given by their "*x*," "*y*," and "*z*" values. Regions of interest are defined in Figure 1. In Figure 4, the volumetric differences of the visual cortex are projected on the cortical surface.

Volumetric Loss in the Pregeniculate Structures

We found a volumetric decrease of the optic nerve ipsilateral to the blind eye, the optic chiasm, and the bilateral optic tracts. These volumetric losses are consistent with a degeneration of the axons from the removed blind eye. Such degeneration in the pregeniculate structures has been observed previously in a pathohistologic study in a single patient who underwent enucleation of one eye 40 years before the study, in which evidence was found for axonal degeneration in the ipsilateral optic nerve relative to the blind eye, in both optic tracts, and in the neuronal laminae corresponding to the enucleated eye in both lateral geniculate nuclei.[33] Our study showed that the results of Beatty et al.[33] are common to monocularly blind patients. However, in contrast to Beatty et al.,[33] we did not find any differences in the lateral geniculate bodies. It could be that the finding of Beatty et al.[33] is specific to their patient, or that the differences in the lateral geniculate bodies are too small or variable to be detected by MRI analysis.

Occipital White Matter Volumetric Increase

We found a few small sections of increased white matter within the optic radiations located close to the region of gray matter volumetric reduction in the superior lateral occipital cortices. The areas of white matter volumetric increase were located within our masks of the optic radiation. However, since the configuration of the largest cluster of increased white matter is oriented vertically rather than horizontally, this cluster might also be part of the vertical occipital fasciculus, which connects the dorsolateral and ventrolateral visual cortices, as recently rediscovered by Yeatman et al.[69] Using diffusion tensor imaging, a number of studies[70–72] have shown that white matter fractional anisotropy increases in various brain areas after learning a specific skill. Therefore, the increase in white matter we found might indicate neural remodeling in monocularly blind patients due to their learning to rely more extensively on alternative cues for estimating depth, for example, based on parallax, texture gradients, or familiar size.

Investigative Ophthalmology & Visual Science

Downloaded from iovs.arvojournals.org on 10/17/2019

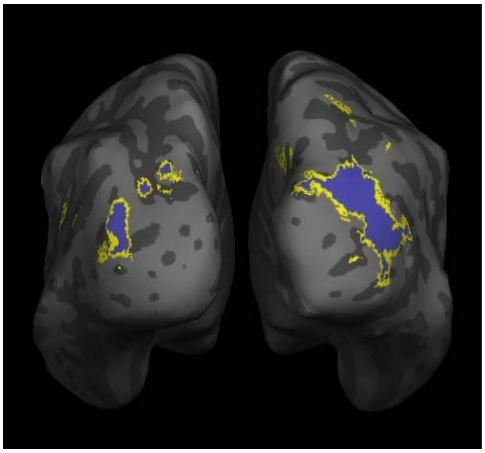

FIGURE 4. Volumetric differences in the ROIs of the visual cortex projected on the cortical surface. The *blue* areas (delineated in *yellow*) highlight the regions in the monocular blind patients that show a significantly lower gray matter volume in the ROIs of the visual cortex than in the healthy controls ($P < 0.05$, uncorrected).

Comparison With Previous Visual Deprivation Studies

Compared to our study, previous structural MRI studies in bilateral blind subjects have found more widespread neuroanatomic changes.[20–31,73] This is to be expected, as in bilateral blind subjects there is a complete lack of visual input, whereas in monocularly blind subjects visual input from the healthy eye sustains largely normal visual functioning. However, in bilateral blind cases, it is much harder to establish the selectivity of functional deprivation, whereas in our study we could.

Furthermore, in a series of studies in monocular blind patients who underwent enucleation early in life, degeneration of the anterior part of the visual system and anatomic changes in visual, auditory, and multisensory cortices are found. Also, motion processing, and spacing and face perception are altered. In contrast to the present study, it is more likely that plasticity occurs in these patients, since the enucleation had taken place at very young age.[35,74–77]

Moreover, previous studies in glaucoma and macular degeneration have found neuroanatomic changes along the entire visual pathway, including changes in the early visual cortex (detectable with current MRI).[5–8,66–68] This is consistent with the fact that these studies have examined patients with binocular visual field defects that overlapped thus causing complete functional deprivation of a region of visual cortex. Therefore, we can conclude that structural changes in the early visual cortex can be caused by functional deprivation but require a complete absence of signals due to either blindness or overlapping bilateral visual field defects.

Comparison Between VBM and SBM Results

The aforementioned volumetric differences were obtained by using VBM. With SBM, we found no differences in cortical thickness, mean curvature, and surface area in either the ROI or the whole-brain analyses. The differences could be caused by the different approaches taken by these two methods: VBM does a voxelwise analysis of the gray and white matter volumes, whereas SBM analyzes the cortical anatomic properties in a surface-based manner. Moreover, the techniques of registration and segmentation of the brains differ substantially between these two methods.

Such discrepancies between VBM and SBM results have been observed before. In accordance with our results, in most of these studies SBM shows no changes in cortical anatomic properties in areas where VBM does reveal differences in gray matter volume.[65,7,78–83] This suggests that VBM may be a more sensitive method to discover differences in volume than SBM is for detecting differences in cortical thickness, mean curvature, and surface area. Nevertheless, SBM might give a more accurate representation of structural differences, as it takes the folded nature of the cortex into account, which VBM does not. Indeed, in some studies,[78,82,83] SBM reveals differences in cortical features in areas where VBM does not reveal changes in gray matter volume.

Limitations and Future Studies

The reduced gray matter volume in the lateral occipital cortex is consistent with a loss of stereopsis and binocular function. While we can be completely certain about the absence of these functions in the monocular blind patients, we could not verify their presence prior to the trauma or operation. However, there is no reason to assume that the low incidence of absence of stereopsis would have been higher in the now-monocular-blind patients than in the normal population. Moreover, we do not have data on eye-dominance in our patients before the loss of their eye. Loss of the dominant or nondominant eye could potentially differentially affect the results, albeit presumably in a very limited manner. Importantly, there is no reason to assume that there is a bias toward the loss of either the dominant or nondominant eye, given the underlying cause (tumor or trauma).

Since the monocular blind subjects were not all blind on the same side, we chose to analyze the optic nerves in two separate groups of blind left eye and blind right eye, which made the subject groups rather small. We also performed the analyses with the MRI images left–right flipped so that the blind side was always on the same side. However, these analyses produced a large number of artifacts in particular at the edges of the brain, which were not solved by randomly flipping half of the images of the healthy controls. Therefore, we were not convinced that when using this approach, the results would only reflect anatomic changes due to monocularity of the patients, and not result from the flipping process. Therefore, we chose to perform the analyses with the unflipped data.

Previous studies have found that, in sighted individuals, the cortical magnification factor (i.e., the distance in millimeters of cortex per degree of visual angle) correlates with visual acuity in V1 (e.g., see Duncan and Boynton[84]). This will not have influenced our results, because in our study the variability in visual acuity was small (owing to the inclusion criterion regarding visual acuity), and the mean visual acuity did not differ between patients and controls. Furthermore, the changes we found were beyond V1.

The finding of decreased gray matter density in the superior lateral occipital cortices could also partly reflect the increased white matter volume in adjacent areas. If the nerve fibers extend from the white matter into the cortex, this might interfere with the gray matter analyses. In this case, the changes in gray matter in the superior lateral occipital cortices might not only represent a decrease in gray matter volume, but also a change in the ratio of gray and white matter in this specific area.

The lateral occipital cortex is a large region in which, among depth perception, also other functions are represented. Functional studies[54,62,63] have shown that depth perception specifically involves dorsal V3. Therefore, a more accurate linkage of the anatomic changes to the functional deprivation

Downloaded from iovs.arvojournals.org on 10/17/2019

would require an analysis specifically of this area. This, in turn, would require exact localization of this area in individual observers, using retinotopic mapping and localizer studies. These additional studies were not performed in the current observers but could be considered in future studies addressing this issue.

As we suggested earlier on, prolonged changes in information use—as a compensation for the loss of stereoscopy—might change the functional connectivity between areas, which in turn might also cause structural changes in connectivity to the superior lateral occipital cortices. It is tempting to speculate on the degree to which differences in compensatory mechanisms might lead to individual differences in gray and white matter alterations. Such effects are too subtle to be picked up by the current methods, which require group comparisons. However, such questions might perhaps be answered in a prospective study, which would allow within-subject analyses and performance of appropriate functional tests in advance.

If—in the future—treatment to restore visual function would become common practice, studies on the relationship between ocular disease, visual function loss, and neuroanatomic changes may give an indication of the chances of success of such a treatment. This notion presumes that regions with more extensive degeneration would be less likely to recover from prolonged functional deprivation and less likely to be able to support restored visual function. This remains to be established.

Conclusions

In this study in monocularly blind patients, we established that the volumes of bilateral superior lateral occipital cortices are reduced, which is most likely caused by the loss of binocular vision and stereopsis. Importantly, we found no evidence for degeneration of the optic radiations and early visual cortex. This indicates that the volumetric reductions in the post-geniculate visual pathways are caused by a selective functional deprivation of the affected areas, rather than by transsynaptic degeneration.

Acknowledgments

The authors thank Anita Sibeijn-Kuiper and Judith Streurman for assistance in MRI acquisition, Remco Renken and Jan-Bernard Marsman for assistance and suggestions regarding the data analysis, Bauke de Jong for suggestions regarding interpretation of results, and Anneke Hooymans for general support for this research.

Supported by the "Junior Scientific Masterclass MD/PhD Programme" of the University Medical Center Groningen and by Stichting Nederlands Oogheelkundig Onderzoek.

Disclosure: **D. Prins**, None; **N.M. Jansonius**, None; **F.W. Cornelissen**, None

References

1. Stingl K, Greppmaier U, Wilhelm B, Zrenner E. Subretinal visual implants. *Klin Monbl Augenheilkd*. 2010;227:940–945.
2. da Cruz L, Coley BF, Dorn J, et al. The Argus II epiretinal prosthesis system allows letter and word reading and long-term function in patients with profound vision loss. *Br J Ophthalmol*. 2013;97:632–636.
3. Van Zeeburg EJT, Maaijwee KJM, Missotten TOAR, Heimann H, Van Meurs JC. A free retinal pigment epithelium-choroid graft in patients with exudative age-related macular degeneration: results up to 7 years. *Am J Ophthalmol*. 2012;153:120–127.
4. MacLaren RE, Groppe M, Barnard AR, et al. Retinal gene therapy in patients with choroideremia: initial findings from a phase 1/2 clinical trial. *Lancet*. 2014;383:1129–1137.
5. Hernowo AT, Boucard CC, Jansonius NM, Hooymans JMM, Cornelissen FW. Automated morphometry of the visual pathway in primary open-angle glaucoma. *Invest Ophthalmol Vis Sci*. 2011;52:2758–2766.
6. Boucard CC, Hernowo AT, Maguire RP, et al. Changes in cortical grey matter density associated with long-standing retinal visual field defects. *Brain*. 2009;132:1898–1906.
7. Hernowo AT, Prins D, Baseler HA, et al. Morphometric analyses of the visual pathways in macular degeneration. *Cortex*. 2014;56:99–110.
8. Plank T, Frolo J, Brandl-Rühle S, et al. Gray matter alterations in visual cortex of patients with loss of central vision due to hereditary retinal dystrophies. *Neuroimage*. 2011;56:1556–1565.
9. Xiao JX, Xie S, Ye JT, et al. Detection of abnormal visual cortex in children with amblyopia by voxel-based morphometry. 2007;143:489–493.
10. Xie S, Gong GL, Xiao JXI, et al. Underdevelopment of optic radiation in children with amblyopia: a tractography study. *Am J Ophthalmol*. 2007;143:642–646.
11. Mendola JD, Conner IP, Roy A, et al. Voxel-based analysis of MRI detects abnormal visual cortex in children and adults with amblyopia. *Hum Brain Mapp*. 2005;25:222–236.
12. Barnes GR, Li X, Thompson B, Singh KD, Dumoulin SO, Hess RF. Decreased gray matter concentration in the lateral geniculate nuclei in human amblyopes. *Invest Ophthalmol Vis Sci*. 2010;51:1432–1438.
13. Prins D, Hanekamp S, Cornelissen FW. Structural brain MRI studies in eye diseases: are they clinically relevant? A review of current findings. *Acta Ophthalmol*. 2016;94:113–121.
14. Cumurcu T, Dorak F, Cumurcu BE, Erbay LG, Ozsoy E. Is there any relation between pseudoexfoliation syndrome and Alzheimer's type dementia? *Semin Ophthalmol*. 2013;28:224–229.
15. Ghiso JA, Doudevski I, Ritch R, Rostagno AA. Alzheimer's disease and glaucoma: mechanistic similarities and differences. *J Glaucoma*. 2013;22(suppl 5):S36–S38.
16. Janssen SF, Gorgels TGMF, Ramdas WD, et al. The vast complexity of primary open angle glaucoma: disease genes, risks, molecular mechanisms and pathobiology. *Prog Retin Eye Res*. 2013;37:31–67.
17. Sivak JM. The aging eye: common degenerative mechanisms between the Alzheimer's brain and retinal disease. *Invest Ophthalmol Vis Sci*. 2013;54:871–880.
18. Tamura H, Kawakami H, Kanamoto T, et al. High frequency of open-angle glaucoma in Japanese patients with Alzheimer's disease. *J Neurol Sci*. 2006;246:79–83.
19. Wostyn P, Audenaert K, De Deyn PP. Alzheimer's disease: cerebral glaucoma? *Med Hypotheses*. 2010;74:973–977.
20. Park H-J, Lee JD, Kim EY, et al. Morphological alterations in the congenital blind based on the analysis of cortical thickness and surface area. *Neuroimage*. 2009;47:98–106.
21. Ptito M, Schneider FCG, Paulson OB, Kupers R. Alterations of the visual pathways in congenital blindness. *Exp Brain Res*. 2008;187:41–49.
22. Wang D, Qin W, Liu Y, Zhang Y, Jiang T, Yu C. Altered white matter integrity in the congenital and late blind people. *Neural Plast*. 2013;2013:128236.
23. Jiang J, Zhu W, Shi F, et al. Thick visual cortex in the early blind. *J Neurosci*. 2009;29:2205–2211.
24. Leporé N, Voss P, Lepore F, et al. Brain structure changes visualized in early- and late-onset blind subjects. *Neuroimage*. 2010;49:134–140.

Downloaded from iovs.arvojournals.org on 10/17/2019

25. Noppeney U, Friston KJ, Ashburner J, Frackowiak R, Price CJ. Early visual deprivation induces structural plasticity in gray and white matter. *Curr Biol*. 2005;15:R488–R490.
26. Pan W-J, Wu G, Li C-X, Lin F, Sun J, Lei H. Progressive atrophy in the optic pathway and visual cortex of early blind Chinese adults: a voxel-based morphometry magnetic resonance imaging study. *Neuroimage*. 2007;37:212–220.
27. Park H-J, Jeong S-O, Kim EY, et al. Reorganization of neural circuits in the blind on diffusion direction analysis. *Neuroreport*. 2007;18:1757–1760.
28. Shimony JS, Burton H, Epstein AA, McLaren DG, Sun SW, Snyder AZ. Diffusion tensor imaging reveals white matter reorganization in early blind humans. *Cereb Cortex*. 2006;16:1653–1661.
29. Shu N, Li J, Li K, Yu C, Jiang T. Abnormal diffusion of cerebral white matter in early blindness. *Hum Brain Mapp*. 2009;30:220–227.
30. Schoth F, Burgel U, Dorsch R, Reinges MHT, Krings T. Diffusion tensor imaging in acquired blind humans. *Neurosci Lett*. 2006;398:178–182.
31. Zhang Y, Wan S, Ge J, Zhang X. Diffusion tensor imaging reveals normal geniculocalcarine-tract integrity in acquired blindness. *Brain Res*. 2012;1458:34–39.
32. Li J, Liu Y, Qin W, et al. Age of onset of blindness affects brain anatomical networks constructed using diffusion tensor tractography. *Cereb Cortex*. 2013;23:542–551.
33. Beatty RM, Sadun AA, Smith L, Vonsattel JP, Richardson EP. Direct demonstration of transsynaptic degeneration in the human visual system: a comparison of retrograde and anterograde changes. *J Neurol Neurosurg Psychiatry*. 1982;45:143–146.
34. Levin N, Dumoulin SO, Winawer J, Dougherty RF, Wandell BA. Cortical maps and white matter tracts following long period of visual deprivation and retinal image restoration. *Neuron*. 2010;65:21–31.
35. Steeves JKE, González EG, Steinbach MJ. Vision with one eye: a review of visual function following unilateral enucleation. *Spat Vis*. 2008;21:509–529.
36. Jenkinson M, Beckmann CF, Behrens TEJ, Woolrich MW, Smith SM. FSL. *Neuroimage*. 2012;62:782–790.
37. Woolrich MW, Jbabdi S, Patenaude B, et al. Bayesian analysis of neuroimaging data in FSL. *Neuroimage*. 2009;45(1 suppl):S173–S186.
38. Smith SM. Fast robust automated brain extraction. *Hum Brain Mapp*. 2002;17:143–155.
39. Zhang Y, Brady M, Smith S. Segmentation of brain MR images through a hidden Markov random field model and the expectation-maximization algorithm. *IEEE Trans Med Imaging*. 2001;20:45–57.
40. Jenkinson M, Smith S. A global optimisation method for robust affine registration of brain images. *Med Image Anal*. 2001;5:143–156.
41. Jenkinson M, Bannister P, Brady M, Smith S. Improved optimization for the robust and accurate linear registration and motion correction of brain images. *Neuroimage*. 2002;17:825–841.
42. Winkler AM, Ridgway GR, Webster MA, Smith SM, Nichols TE. Permutation inference for the general linear model. *Neuroimage*. 2014;92:381–397.
43. Ségonne F, Dale AM, Busa E, et al. A hybrid approach to the skull stripping problem in MRI. *Neuroimage*. 2004;22:1060–1075.
44. Sled JG, Zijdenbos AP, Evans AC. A nonparametric method for automatic correction of intensity nonuniformity in MRI data. *IEEE Trans Med Imaging*. 1998;17:87–97.
45. Fischl B, Liu A, Dale AM. Automated manifold surgery: constructing geometrically accurate and topologically correct models of the human cerebral cortex. *IEEE Trans Med Imaging*. 2001;20:70–80.
46. Ségonne F, Pacheco J, Fischl B. Geometrically accurate topology-correction of cortical surfaces using nonseparating loops. *IEEE Trans Med Imaging*. 2007;26:518–529.
47. Dale AM, Fischl B, Sereno MI. Cortical surface-based analysis, I: segmentation and surface reconstruction. *Neuroimage*. 1999;9:179–194.
48. Fischl B, Sereno MI, Dale AM. Cortical surface-based analysis. II: inflation, flattening, and a surface-based coordinate system. *Neuroimage*. 1999;9:195–207.
49. Fischl B, Sereno MI, Tootell RB, Dale AM. High-resolution intersubject averaging and a coordinate system for the cortical surface. *Hum Brain Mapp*. 1999;8:272–284.
50. Desikan RS, Ségonne F, Fischl B, et al. An automated labeling system for subdividing the human cerebral cortex on MRI scans into gyral based regions of interest. *Neuroimage*. 2006;31:968–980.
51. Fischl B, van der Kouwe A, Destrieux C, et al. Automatically parcellating the human cerebral cortex. *Cereb Cortex*. 2004;14:11–22.
52. Bürgel U, Schormann T, Schleicher A, Zilles K. Mapping of histologically identified long fiber tracts in human cerebral hemispheres to the MRI volume of a reference brain: position and spatial variability of the optic radiation. *Neuroimage*. 1999;10:489–499.
53. Bürgel U, Amunts K, Hoemke L, Mohlberg H, Gilsbach JM, Zilles K. White matter fiber tracts of the human brain: three-dimensional mapping at microscopic resolution, topography and intersubject variability. *Neuroimage*. 2006;29:1092–1105.
54. Ip IB, Minini L, Dow J, Parker AJ, Bridge H. Responses to interocular disparity correlation in the human cerebral cortex. *Ophthalmic Physiol Opt*. 2014;34:186–198.
55. Ban H, Preston TJ, Meeson A, Welchman AE. The integration of motion and disparity cues to depth in dorsal visual cortex. *Nat Neurosci*. 2012;15:636–643.
56. Minini L, Parker AJ, Bridge H. Neural modulation by binocular disparity greatest in human dorsal visual stream. *J Neurophysiol*. 2010;104:169–178.
57. Brouwer GJ, van Ee R, Schwarzbach J. Activation in visual cortex correlates with the awareness of stereoscopic depth. *J Neurosci*. 2005;25:10403–10413.
58. Welchman AE, Deubelius A, Conrad V, Bülthoff HH, Kourtzi Z. 3D shape perception from combined depth cues in human visual cortex. *Nat Neurosci*. 2005;8:820–827.
59. Neri P, Bridge H, Heeger DJ. Stereoscopic processing of absolute and relative disparity in human visual cortex. *J Neurophysiol*. 2004;92:1880–1891.
60. Rutschmann RM, Greenlee MW. BOLD response in dorsal areas varies with relative disparity level. *Neuroreport*. 2004;15:615–619.
61. Backus BT, Fleet DJ, Parker AJ, Heeger DJ. Human cortical activity correlates with stereoscopic depth perception. *J Neurophysiol*. 2001;86:2054–2068.
62. Baecke S, Lützkendorf R, Tempelmann C, et al. Event-related functional magnetic resonance imaging (efMRI) of depth-by-disparity perception: additional evidence for right-hemispheric lateralization. *Exp Brain Res*. 2009;196:453–458.
63. Goncalves NR, Ban H, Sánchez-Panchuelo RM, Francis ST, Schluppeck D, Welchman AE. 7 tesla FMRI reveals systematic functional organization for binocular disparity in dorsal visual cortex. *J Neurosci*. 2015;35:3056–3072.
64. Culham JC, Kanwisher NG. Neuroimaging of cognitive functions in human parietal cortex. *Curr Opin Neurobiol*. 2001;11:157–163.

Investigative Ophthalmology & Visual Science

Downloaded from iovs.arvojournals.org on 10/17/2019

65. Prins D, Plank T, Baseler HA, et al. Surface-based analyses of anatomical properties of the visual cortex in macular degeneration. *PLoS One*. 2016;11:e0146684.
66. Chen WW, Wang N, Cai S, et al. Structural brain abnormalities in patients with primary open-angle glaucoma: a study with 3T MR imaging. *Invest Ophthalmol Vis Sci*. 2013;54:545–554.
67. Li C, Cai P, Shi L, et al. Voxel-based morphometry of the visual-related cortex in primary open angle glaucoma. *Curr Eye Res*. 2012;37:794–802.
68. Williams AL, Lackey J, Wizov SS, et al. Evidence for widespread structural brain changes in glaucoma: a preliminary voxel-based MRI study. *Invest Ophthalmol Vis Sci*. 2013;54:5880–5887.
69. Yeatman JD, Weiner KS, Pestilli F, Rokem A, Mezer A, Wandell BA. The vertical occipital fasciculus: a century of controversy resolved by in vivo measurements. *Proc Natl Acad Sci U S A*. 2014;111:E5214–E5223.
70. Fields RD. Neuroscience: change in the brain's white matter. *Science*. 2010;330:768–769.
71. Scholz J, Klein MC, Behrens TEJ, Johansen-Berg H. Training induces changes in white-matter architecture. *Nat Neurosci*. 2009;12:1370–1371.
72. Schlegel AA, Rudelson JJ, Tse PU. White matter structure changes as adults learn a second language. *J Cogn Neurosci*. 2012;24:1664–1670.
73. Noppeney U. The effects of visual deprivation on functional and structural organization of the human brain. *Neurosci Biobehav Rev*. 2007;31:1169–1180.
74. Steeves JKE, González EG, Gallie BL, Steinbach MJ. Early unilateral enucleation disrupts motion processing. *Vision Res*. 2002;42:143–150.
75. Kelly KR, McKetton L, Schneider KA, Gallie BL, Steeves JKE. Altered anterior visual system development following early monocular enucleation. *Neuroimage Clin*. 2014;4:72–81.
76. Kelly KR, DeSimone KD, Gallie BL, Steeves JKE. Increased cortical surface area and gyrification following long-term survival from early monocular enucleation. *Neuroimage Clin*. 2015;7:297–305.
77. Kelly KR, Gallie BL, Steeves JKE. Impaired face processing in early monocular deprivation from enucleation. *Optom Vis Sci*. 2012;89:137–147.
78. Bridge H, von dem Hagen E, Davies G, et al. Changes in brain morphology in albinism reflect reduced visual acuity. *Cortex*. 2014;56:64–72.
79. von Glehn F, Jarius S, Cavalcanti Lira RP, et al. Structural brain abnormalities are related to retinal nerve fiber layer thinning and disease duration in neuromyelitis optica spectrum disorders. *Mult Scler*. 2014;20:1189–1197.
80. Palaniyappan L, Liddle PF. Differential effects of surface area, gyrification and cortical thickness on voxel based morphometric deficits in schizophrenia. *Neuroimage*. 2012;60:693–699.
81. Voets NL, Hough MG, Douaud G, et al. Evidence for abnormalities of cortical development in adolescent-onset schizophrenia. *Neuroimage*. 2008;43:665–675.
82. Whitwell JL, Tosakulwong N, Weigand SD, et al. Does amyloid deposition produce a specific atrophic signature in cognitively normal subjects? *Neuroimage Clin*. 2013;2:249–257.
83. Lyoo IK, Sung YH, Dager SR, et al. Regional cerebral cortical thinning in bipolar disorder. *Bipolar Disord*. 2006;8:65–74.
84. Duncan RO, Boynton GM. Cortical magnification within human primary visual cortex correlates with acuity thresholds. *Neuron*. 2003;38:659–671.

Investigative Ophthalmology & Visual Science

Downloaded from iovs.arvojournals.org on 10/17/2019